Plant Physiol. (1995) 109: 393–407

Histones of *Chlamydomonas reinhardtii*[1]

Synthesis, Acetylation, and Methylation

Jakob Harm Waterborg*, Anthony James Robertson, Dalida Laura Tatar, Corina Marilena Borza, and James Ronald Davie

School of Biological Sciences, University of Missouri-Kansas City, 5100 Rockhill Road, Kansas City, Missouri 64110–2499 (J.H.W., A.J.R., D.L.T., C.M.B.); and Department of Biochemistry and Molecular Biology, Faculty of Medicine, University of Manitoba, 770 Bannatyne Avenue, Winnipeg, Manitoba Canada R3E 0W3 (J.R.D.)

Histones of the green alga *Chlamydomonas reinhardtii* were prepared by a new method and fractionated by reversed-phase high-performance liquid chromatography. Acid-urea-Triton gel analysis and tritiated acetate labeling demonstrated high levels of steady-state acetylation for the single histone H3 protein, in contrast to low levels on histones H4 and H2B. Twenty percent of histone H3 is subject to dynamic acetylation with, on average, three acetylated lysine residues per protein molecule. Histone synthesis in light-dark-synchronized cultures was biphasic with pattern differences between two histone H1 variants, between two H2A variants, and between H2B and ubiquitinated H2B. Automated protein sequence analysis of histone H3 demonstrated a site-specific pattern of steady-state acetylation between 7 and 17% at five of the six amino-terminal lysines and of monomethylation between 5 and 81% at five of the eight amino-terminal lysines in a pattern that may limit dynamic acetylation. An algal histone H3 sequence was confirmed by protein sequencing with a single threonine as residue 28 instead of the serine^{28}-alanine^{29} sequence, present in all other known plant and animal H3 histones.

Acetylation of histones modulates histone interaction with DNA when nucleosomes are assembled on newly replicated DNA, when chromatin is transcribed, or when histones are displaced by protamines during spermatogenesis (for recent reviews, see Van Holde, 1989; Csordas, 1990; Grunstein, 1990). The conserved amino-terminal domains of histones H3 and H4, with multiple acetylated Lys's in transcriptionally active chromatin (Matthews and Waterborg, 1985), appear especially important. Experiments in yeast (Megee et al., 1990; Durrin et al., 1991; Clarke et al., 1993), *Physarum* (Waterborg et al., 1983; Pesis and Matthews, 1986), *Tetrahymena* (Chicoine et al., 1986), *Drosophila* (Munks et al., 1991), and higher animals (Couppez et al., 1987; Turner and Fellows, 1989; Thorne et al., 1990) and plants (Waterborg, 1992b) have in recent years demonstrated that acetylation of specific Lys's within the amino-terminal domain of histone H4 are required for the modulation of chromatin structure in transcription and replication. The same general conclusion also appears valid for acetylation of histone H3 in yeast (Mann and Grunstein, 1992), *Tetrahymena* (Chicoine et al., 1986), and humans (Thorne et al., 1990). The preponderance of acetylation of histone H3 over histone H4 in plants (Waterborg et al., 1989; Waterborg, 1991, 1992a), also with a nonrandom distribution of Lys acetylation (Waterborg, 1990), suggests that histone H3, centrally located within the nucleosome (Arents et al., 1991; Arents and Moudrianakis, 1993), is more intensely involved in the modulation of transcribing chromatin in plants than in animals. Indirect support for this view was obtained from the remarkably high rate of turnover of histone H3 in transcriptionally active chromatin of higher plants (Waterborg, 1993b). To evaluate the validity of this observation for a wider range of species than just angiosperms, the analysis of histone H3 in the green alga *Chlamydomonas reinhardtii* was initiated.

A recent analysis of the chromatin of *Chlamydomonas* has shown that a full complement of five histones packages DNA into an apparently typical higher eukaryotic chromatin with a nucleosomal repeat length of 189 bp (Morris et al., 1990). In recent years, several complete histone gene clusters of *C. reinhardtii* have been cloned. Sequences for three complete genomic genes for each of the four core histones have been determined (GenBank accession Nos. U16724, U16725, U16726, and U16826) (Fabry et al., 1995).

This study presents a new method to prepare histone proteins from *Chlamydomonas*, an analysis of histone synthesis in the cell cycle, and the analysis of posttranscriptional modification of histone H3 by acetylation and methylation, including site specificity.

MATERIALS AND METHODS

Algal Cell Culture

Chlamydomonas reinhardtii, CC-400 *cw-15* mt$^+$ clone DG-1, a cell-wall-deficient strain, was obtained from the Chlamydomonas Genetics Center at Duke University (Durham, NC) and grown at 28°C to a density of 7×10^6

[1] This work was supported by National Science Foundation grant No. DCB-9118999 and by an award by the University of Missouri Research Board to J.H.W.

* Corresponding author; e-mail waterborg@cctr.umkc.edu; fax 1–816–235–5158.

Abbreviations: AUT, acetic acid-urea-Triton X-100; GuCl, guanidine hydrochloride; uH2B, ubiquitinated H2B.

cells/mL as mixotrophic shaking suspension culture in Sueoka's high-salt medium with ammonium acetate and Hutner trace elements and supplemented with yeast extract at 4 g/L and bactotryptone at 0.5 g/L (Harris, 1989). Phototrophic cultures were grown at 30°C and white light at 75 μE PAR m^{-2} s^{-1} to a density between 1 and 5 $\times$ 10^6 cells/mL in 800-mL glass cylinders (4 cm in diameter) by bubbling 5% CO_2-enriched air through Sueoka's high-salt minimal medium (Harris, 1989). The light flux was chosen to obtain under these culture conditions a single doubling of cells, early during the dark phase of the 12-h light and 12-h dark synchronization regimen. Cell density was measured by hemacytometer counting. The time of cell division was estimated in these cell wall-less mutants from the cell density and by visual scoring of the percentage of cells with nonglobular cell morphology and cells in clusters. These latter include cells during the initiation of the process of cell division and cells in bicellular associations, the early result of completion of cell division. Semistable palmelloid cell clusters are not produced in this mutant.

Phototrophic cell cultures in high-salt minimal medium and at a cell density between 1 and 5 $\times$ 10^6 cells/mL were labeled with [^{3}H]acetate (6 Ci/mmol, New England Nuclear) for 5 min at 10 μCi or for 2 h at 2.5 μCi/mL culture. Isotope-specific incorporations were compared in nonsynchronized (continuous light) phototrophic cultures, incubated for 3 h with 5 μCi/mL [^{3}H]acetate or with 0.5 μCi/mL [1-^{14}C]acetate (57 mCi/mmol, New England Nuclear). Incorporation of label was terminated by rapid cooling of the cultures in melting ice and collection of cells in a refrigerated centrifuge.

Histone mRNA Analysis

Total cellular RNA was extracted from approximately 3 $\times$ 10^7 cells and collected by centrifugation for 10 min at 7000*g*, with 2.5 mL of TRIzol, essentially as described by Gibco-BRL, as modified by Kapros and Waterborg (1995). Northern blots (Sambrook et al., 1989) were hybridized with digoxygenin-substituted probes, prepared from the subcloned coding regions of histones H3 and H4 of a single histone gene cluster of *C. reinhardtii*, as described in technical protocol No. 1093657 (1988) for the Genius system by Boehringer Mannheim. Parts of this genomic histone cluster (*ch-iii*, GenBank accession No. U16725) were kindly provided by Clark Ford (Iowa State University). The probe for histone H3 was prepared using a 433-bp *Sty*I fragment of the H3 gene clone B1 in a pBS+ vector that starts at +68, relative to the Met start codon, with a 363-bp coding sequence for histone H3. The hybridization probe for histone H4 was prepared from a 356-bp *Bam*HI-*Nco*I fragment of the H4-containing *Bam*HI-*Xho*I fragment of clone A3, subcloned into pGEM7zf(+).

Nuclear Isolation and Preparation of Histones

Nuclei were isolated according to the method of Keller et al. (1984), as modified by Shimogawara and Muto (1992) with the following changes. Cells were collected by centrifugation for 10 min at 7,000*g*, resuspended in 0.6 M Suc in 20 mM Hepes, 10 mM $CaCl_2$, 10 mM $MgCl_2$, 2.5 mM spermidine, 0.75 mM spermine, 5 mM 2-mercaptoethanol, 0.5 mM PMSF, adjusted with KOH to pH 7.6 (buffer A), and lysed by the addition of Triton X-100 to 1% (w/v). Two volumes of 2.0 M Suc in buffer A were added to the lysate. Nuclei were pelleted by centrifugation for 1 h at 18,000*g*, resuspended in 1.8 M Suc in buffer A, and collected by a spin of 30 min at 32,000*g*.

Histones were extracted from the nuclear pellet by an adaptation of the method developed for *Physarum polycephalum* (Mende et al., 1983) and modified for plants (Waterborg, 1990). Briefly, 10^{10} nuclei with approximately 1.2 mg of DNA (Harris, 1989), obtained from mixotrophic cultures, were lysed on ice by sonication in 1 mL of 40% (w/v) GuCl in 1 mM 2-mercaptoethanol, 0.1 M potassium phosphate buffer, pH 6.8 (40% GuCl buffer). The homogenate was clarified by centrifugation for 10 min at 30,000*g*, nucleic acids and acidic proteins were removed by a similar centrifugation after acidification on ice to 0.25 N HCl, and solubilized histones were adsorbed overnight at room temperature to 1.2 mL of Bio-Rex-70 resin (Bio-Rad) in 5% GuCl buffer. The resin was allowed to settle from the turbid suspension and washed extensively batchwise in 5% GuCl buffer. Histones were desorbed by 8 column volumes of 40% GuCl buffer, dialyzed exhaustively against 2.5% (v/v) acetic acid containing 1 mM 2-mercaptoethanol, and lyophilized until dry. The same method using 0.1 mL of resin was used to prepare histones from nuclei obtained from 10^7 cells of photosynthetic culture.

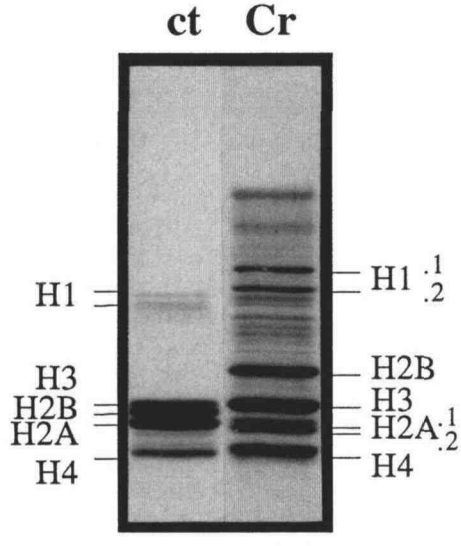

Figure 1. SDS gel analysis of *Chlamydomonas* histones. Total nuclear histone extract from 2.5 $\times$ 10^8 cells in a mixotrophic culture of *C. reinhardtii* (Cr) was electrophoresed from top to bottom in an SDS-polyacrylamide gel and stained with Coomassie blue, in parallel with calf thymus histones (ct). The identity of calf histones is given. The *Chlamydomonas* histone bands are marked as established by Morris et al. (1990), with variant nomenclature as established in this paper.

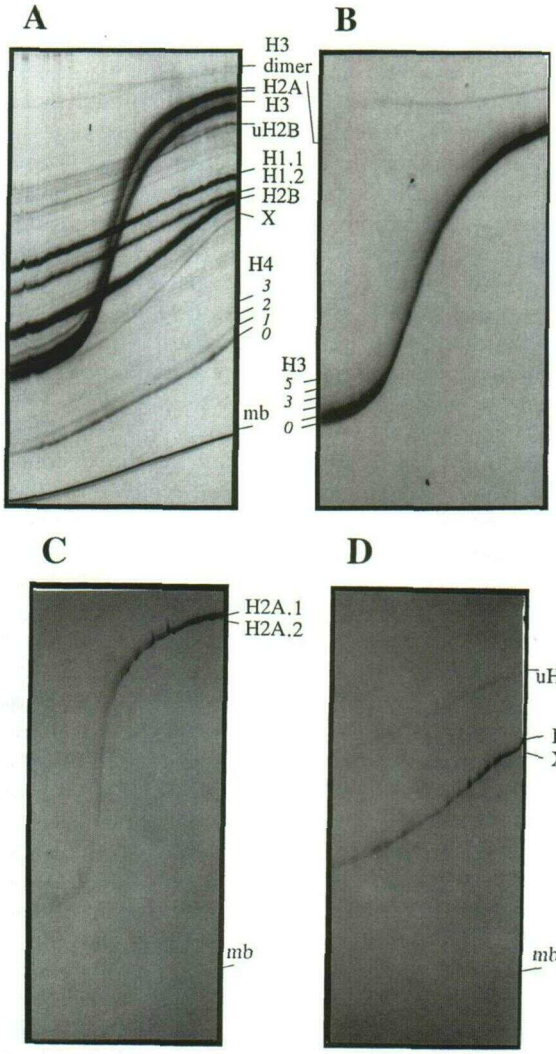

Figure 2. AUT gradient gel electrophoresis. A, Total nuclear histone extract from 6×10^9 cells in mixotrophic culture of *Chlamydomonas*. Electrophoresis was from top to bottom. The linear gradient of Triton X-100 ranged from 0 mM at the left side of the gel to 10 mM at the right side. The gel was stained with Coomassie brilliant blue. mb marks the mobility of methylene blue dye that migrates in the discontinuous buffer front of this gel system. The electrophoretic mobility of all charged molecular species is reduced from left to right inside the gel and reflects a gradient of glycerol from 0 to 10% (v/v), which is used to stabilize the gradient gel prior to acrylamide polymerization. A mobility pattern, independent of the concentration of Triton X-100, is observed for all nonhistone proteins and for linker histones H1.1 and H1.2. Depending on the concentration of Triton X-100, the electrophoretic mobility of the core histones is increasingly retarded for histone H4 (apparent acetylation levels of 0 to 3 acetyl-Lys residues are marked), histone H2B and uH2B, histone H3, and the two closely migrating H2A histones (H2A). A small amount of H3 dimerization (H3 dimer) was observed. The faint trace of putative ubiquitinated H2A with a slightly higher gel mobility than uH2B at 0 mM Triton is not marked. The identity of protein X, by mobility shift identified as a core histone, most likely a form of H2B, has not yet been established. B, Coomassie blue-stained histone H3, pooled after HPLC fractionation (Fig. 3) of the histone preparation of A and electrophoresed in an AUT gradient gel as shown in A. Charge-modified forms are marked as levels of acetylation. C, Coomassie blue-stained histone H2A forms, pooled as the H2A peak after HPLC fractionation (Fig. 3), electrophoresed in an AUT gradient gel as shown in A. The two parallel bands of H2A variants H2A.1 and H2A.2 and the mobility of methylene blue (mb) dye are indicated. D, Coomassie blue-stained histone H2B forms, pooled as the combined H2B and uH2B peak after HPLC fractionation (Fig. 3), electrophoresed in an AUT gradient gel as shown in A. The bands of H2B, uH2B, methylene blue dye (mb), and a small amount of unidentified protein X, marked as in A, are indicated.

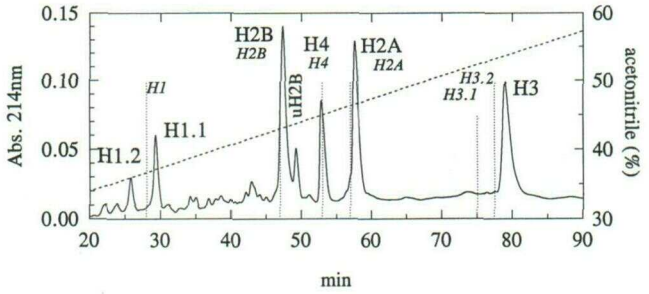

Figure 3. Reversed-phase HPLC fractionation of *Chlamydomonas* histones. A_{214} pattern obtained from 250 μg of crude nuclear histones, extracted from 2×10^9 cells, fractionated by reversed-phase HPLC using a linear gradient from 30 to 60% acetonitrile (broken line), as described in "Materials and Methods." The major *A* peaks in this pattern were all identified as *Chlamydomonas* histones, as described, and are marked by their names. Dotted lines, labeled with histone names in italics, mark the elution times for alfalfa histones in a parallel, chromatographic fractionation.

Purification and Analysis of Histone Proteins

Histones were solubilized in 1 M acetic acid, 7.2 M urea as described previously (Waterborg, 1990). Up to 1.5 mg of protein were fractionated by reversed-phase HPLC on a Zorbax Protein-Plus (4.6 × 250 mm) column from MAC-MOD Analytical, Inc. (Chadds Ford, PA), developed at a flow rate of 1 mL/min with a 20%/h gradient of 30 to 60% (v/v) acetonitrile in water. All solutions contained 0.1% (v/v) TFA. The A_{214} of the column eluent was monitored, and 1-mL fractions were collected. Elution of radioactivity was monitored by liquid scintillation counting of 0.1-mL aliquots. To prevent protein oxidation, all fractions were made 1 mM 2-mercaptoethanol. Selected fractions were pooled, aliquoted, and lyophilized until dry. All histones were analyzed by SDS and AUT gel electrophoresis (Waterborg, 1990). Ubiquitination of histone H2B was identified by western analysis of total and HPLC-fractionated histones (0.5-mL fractions). Histones were electrophoresed on one-dimensional, continuous AUT gels (acetic acid, 6.7 M urea, 0.375% [w/v] Triton X-100, 15% polyacrylamide) as previously described (Nickel et al., 1989). The gels were stained with Coomassie blue or transferred to nitrocellulose and immunochemically stained for ubiquitin with an anti-ubiquitin IgG as described previously (Delcuve and Davie, 1992). Discontinuous AUT gels with a transverse gradient from 0 to 10 mM Triton X-100 were prepared and run as described previously (Waterborg, 1991, 1992a). Calf thymus histones from Worthington Biochemical Corp., Inc. (Freehold, NJ) were included in all gels with multiple lanes as reference proteins. Gel fluorography and densitometric

analysis were performed as described previously (Mende et al., 1983; Waterborg, 1990, 1991, 1992a). Histone H3, purified from mixotrophic culture, was solubilized in 6 N HCl prior to amino acid analysis and in 0.1% (v/v) TFA in water prior to protein sequencing (Waterborg, 1990). Purified H3 (0.85 nmol) was subjected to automated Edman degradation sequencing for 50 cycles as described previously (Waterborg, 1990) with extended Pro cleavage at residues 16, 30, 38, and 43. Additional details of amino acid analysis and protein sequencing with elution and quantitation of acetylated and methylated Lys derivatives have been described elsewhere (Waterborg, 1990).

RESULTS

Chlamydomonas Histone Analysis by Gel Electrophoresis and Reversed-Phase HPLC

The identity of histones in *Chlamydomonas* has been established by Morris et al. (1990) by electrophoretic comparisons of gel-purified histones and their protease fragmentation patterns with known histones and by amino acid analyses. This study established that, within a nucleosome of fairly typical characteristics, *Chlamydomonas* contains two forms of linker histone H1 and two forms of core histone H2A, which all differ in size, in addition to single species of core histones H2B, H3, and H4 (Morris et al., 1990). The method that was used with success by these researchers to extract histones was one originally developed for *Physarum*. In the past, we developed a different method to prepare *Physarum* histones that better preserved histones and their modifications and excluded carbohydrates from co-purification (Mende et al., 1983). This method has more recently been applied with success to prepare histones from higher plants (Waterborg et al., 1987; Waterborg, 1991, 1992a). Preparation of histones from isolated nuclei of *Chlamydomonas* produced an SDS protein pattern (Fig. 1) (Morris et al., 1990).

Inspection of these histones after AUT electrophoresis in a gel system with a transverse gradient of Triton X-100 (Waterborg et al., 1987; Waterborg, 1992a) confirmed the presence of two histone H1 linker histone forms of different size, which, according to the established convention, were named H1.1 and H1.2, in the order of increasing gel mobility. Preliminary identification of core histones can be obtained in this gel system because core histones show typically histone species-specific differences in their affinity for Triton and thus a histone-specific reduction in gel mobility. Affinity for Triton typically increases from low for histone H4, to moderate for H2B, to intermediate or high for H3, and to high or very high for H2A (Franklin and Zweidler, 1977; Waterborg et al., 1987). This same relationship, substantiated by further analyses shown below, has been confirmed for *Chlamydomonas*. As in most other species, charge modification by Lys acetylation, confirmed below by acetate-labeling experiments, was clearly observed for histones H3 and H4 (Fig. 2A).

The tentative identification of all histones was confirmed by fractionation of a crude histone preparation by reversed-phase HPLC (Fig. 3) into individual peaks and their analysis by SDS gel electrophoresis (results not shown). The small linker histone H1.2 eluted prior to the larger histone H1.1 variant form, at a concentration of acetonitrile typical for other linker histones. It was assumed that the two forms represented products from distinct genes that differed in size rather than proteolytically related forms of a single protein. This was based on the failure to detect proteolysis or interconversion between the forms upon storage. The histone extraction method used was designed specifically to prevent proteolytic damage and enzymatic loss of protein modifications (Mende et al., 1983). The assumption has subsequently been substantiated by the differential pattern of linker histone variant synthesis in the cell cycle, which is described later.

AUT gel analysis of individual and pooled HPLC peaks was performed to study, in more detail, the core histones of *Chlamydomonas*. The single H2A peak, which eluted very much like the higher plant alfalfa H2As (Fig. 3), contained the two forms that differed slightly in apparent size in SDS (Morris et al., 1990) (results not shown) and AUT gradient gel electrophoresis (Fig. 2C). By convention, the two forms were named H2A.1 and H2A.2, in the order of increasing mobility in AUT gels.

Chlamydomonas and alfalfa histone H4 co-eluted upon reversed-phase HPLC fractionation (Fig. 3) and showed qualitatively very similar patterns of charge modifications (Fig. 2A) (Waterborg et al., 1987, 1989). Pulse labeling in vivo with radioactive acetate (results not shown) has subsequently confirmed that, as in other species, the basis of the differently charged forms is due to distinct levels of Lys acetylation (Fig. 2A). In the HPLC elution pattern, the *A* peak for histone H4 has consistently been low (Fig. 3). Coomassie blue staining of AUT gels also suggested a reduced amount of histone H4 in the total nuclear histone extract, relative to the other histone species (Fig. 2A). However, when assayed by Coomassie blue staining of SDS gels, the expected, stochiometric amount of histone H4 appeared present in the histone extract produced (Fig. 1) and in the HPLC fractions where Coomassie blue staining in SDS gels consistently gave stronger H4 staining than in AUT gels (results not shown). Thus, the HPLC pattern in Figure 3 does not represent a relative failure to extract histone H4 from nuclei or a preferential loss in any step through HPLC. The basis for the differential staining of *Chlamydomonas* histone H4 in the two gel systems is unknown.

The peak of histone H2B was consistently followed by a smaller peak (Fig. 3) that contained a protein with a higher molecular weight than H2B and two smaller protein species (Fig. 4A). The larger of these two was tentatively identified as a minor form of histone H2B, based on its affinity for Triton in gradient acid-urea gel electrophoresis (Fig. 2D). In AUT gel electrophoresis it has a mobility virtually identical with that of the major H2B form (Fig. 4B), and this has prevented determination of its abundance relative to the major H2B protein. The smallest, least abundant of the two smaller protein species appeared to be a form of H4 by size (Fig. 4A), charge, and apparent acetylation (Fig. 4B). The high-molecular-weight component in

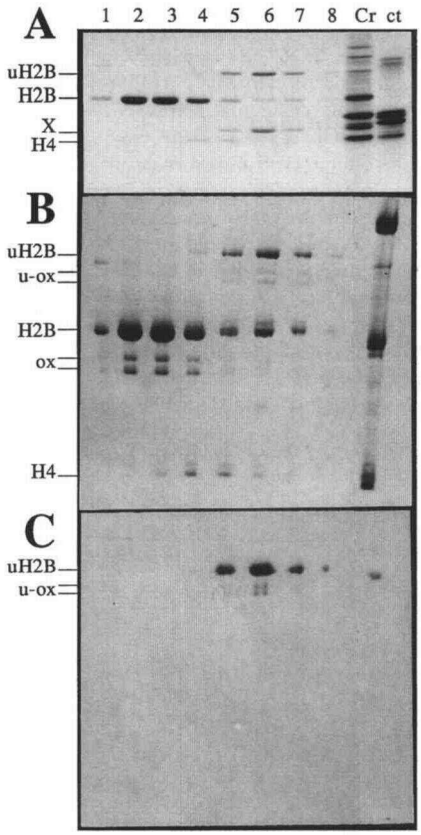

Figure 4. Identification of ubiquitinated histone H2B. Electrophoretic gel analysis of total histones from mixotrophic culture and of eight 0.5-mL HPLC fractions (lanes 1–8), spanning the elution of the main H2B elution peak and following smaller peak (Fig. 3). A, Coomassie blue-stained SDS polyacrylamide gel with 5 μg of calf thymus histones (ct), 10 μg of total (Cr), and 160 μg of HPLC-fractionated (1–8) *Chlamydomonas* histones. *Chlamydomonas* uH2B, H2B, a minor H2B form (X), and H4 are marked. For the identity of other bands, see Figure 1. B, Coomassie blue-stained continuous AUT polyacrylamide gel with 9 μg of total and 90 μg of fractionated histones. ox marks partially oxidized H2B and uH2B artificial forms (Waterborg et al., 1989). C, Anti-ubiquitin western blot of an AUT gel as in B.

the trailing peak was identified as uH2B by western analysis of AUT gels with anti-ubiquitin antibodies (Fig. 4C). The abundance of uH2B was estimated as 29 ± 3% (n = 21) on the basis of UV *A* upon HPLC elution (Fig. 3), likely an overestimate due to the smaller co-eluting protein species (Fig. 4A), and as 13 ± 1% (n = 3) or 18 ± 4% (n = 11) by staining with Coomassie blue in SDS (Fig. 4A) or AUT gels (Figs. 2D and 4B), respectively. Shimogawara and Muto (1992) purified and partially sequenced a nuclear protein from *Chlamydomonas*, which was found to be a conjugate between H2B and ubiquitin. Ubiquitination of H2B histones has been observed in a large variety of species and in animal systems is typically observed at a lower abundance than ubiquitinated H2A (Wu et al., 1986). In *Chlamydomonas* only a faint trace of a core histone protein species with a high affinity for Triton like H2A and with a molecular weight almost as high as uH2B has been observed (Fig. 2A). Thus, ubiquitination of H2B and H2A core histones appears to exist in *Chlamydomonas* but with a clear preponderance for histone H2B.

Histone H3 elutes as a single, homogeneous peak in reversed-phase HPLC with a higher apparent hydrophobicity than alfalfa H3.1 and H3.2 histone variants (Fig. 3). In comparison with these plant histones, the affinity for Triton in AUT gel electrophoresis is also higher (Fig. 5A) and very similar to that of mammalian H3.1 histone (Franklin and Zweidler, 1977). In AUT gel electrophoresis five distinct, charge-modified forms are observed above the main band of *Chlamydomonas* histone H3 (Figs. 2B and 5). This is the same value as the maximum level of histone H3 acetylation in higher plant H3 histones (Waterborg, 1990). This pattern suggests an average level of 0.75 acetylated Lys residues per histone H3 (Table I). However, the quantitative distribution of the acetylated forms in *Chlamydomonas* histone H3 is rather unusual with an abundance of nonacetylated and highly acetylated forms and underrepresentation of di- and triacetylated H3 when compared with a more typical pattern of acetylation in histone H3 species in plants (Fig. 5B) and animals.

Radioactive Acetate Incorporation into Histones

The analyses presented above were all performed on histones prepared from algae grown under mixotrophic growth conditions, in light, and with acetate as an additional carbon source. The identity of the prominent charge-

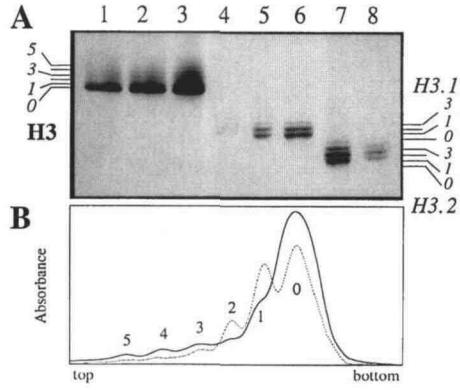

Figure 5. Comparison of AUT gel electrophoresis of *Chlamydomonas* and alfalfa histone H3. A, *Chlamydomonas* histone H3, purified by HPLC (Fig. 3), was electrophoresed at three levels of loading (relative amounts 3, 5, and 10) in lanes 1, 2, and 3, in parallel with histone H3 variants of alfalfa, separated by reversed-phase HPLC into fractions containing histone H3.1 and H3.2 (Waterborg, 1990) and electrophoresed in lanes 4 to 8. The AUT gel was stained by Coomassie blue. The mobility of non- through penta-acetylated *Chlamydomonas* H3 is marked on the left. The mobilities of non- through triacetylated forms of alfalfa H3.1 (top) and H3.2 (bottom) are indicated on the right. B, Densitometric registration of Coomassie blue dye bound to *Chlamydomonas* histone H3 in lane 2 of A (continuous line) with the top of the AUT gel at left. The numerical analysis of this pattern is shown in Table I, first column. As a dotted line the pattern of alfalfa histone H3.2 in lane 7 of A is shown. The average, steady-state acetylation of this alfalfa H3.2 histone was similar to that of the *Chlamydomonas* H3 at 0.62 acetylated Lys's per histone molecule.

Table I. *Analysis of histone H3 acetylation by AUT gel electrophoresis*

The extent of histone H3 acetylation was determined by quantitative densitometry of AUT gels. No. indicates the number of acetylated Lys residues per histone molecule. The average number of acetylated Lys residues per histone H3 protein (AcLys/H3) was calculated from the distribution of acetylation levels in each column. Second column, Steady-state acetylation in Coomassie blue-stained AUT gels with histone H3 protein prepared from mixotrophic cultures (Mix) (Fig. 5). Third column, Average ± SD steady-state acetylation in Coomassie blue-stained AUT gels of histone H3, purified from three independent, phototrophic cultures (Photo). Fourth column, Distribution of radioactivity, determined by densitometry of AUT gel fluorographs, for histone H3 purified from light-dark-synchronized, phototrophic cultures that were incubated for 5 min with [^{3}H]acetate after 4 h of light (L = 4 h) (Fig. 10A). Fifth column, Results, as in fourth column, obtained upon labeling after 4 h of dark (D = 4 h) (Fig. 10C). Sixth column, Calculated distribution of acetate label into amino acids that were incorporated into newly synthesized histone H3 protein during a 5-min pulse label (Fig. 10C). Dashes indicate the absence of detectable amounts of acetylation. Seventh column, Calculated average ± SD distribution, of acetate label incorporated into acetylated Lys by posttranslational side chain modification (AcLys). The data were derived from the fourth and fifth columns (Fig. 10, A and C) and were adjusted for label incorporation into amino acids (sixth column). It was assumed that no label from acetate could be incorporated into nonacetylated histone H3 by posttranslational modification (≡ 0%). Eighth column, Calculation of steady-state acetylation of histone H3 molecules, subject to the posttranslational, dynamic acetylation, which is detected by acetate pulse labeling (seventh column). This calculation was based on the histone H3 protein preparations shown in the second and third columns, used the distribution of acetylation of newly synthesized histone H3 of the sixth column and assumed that nonacetylated histone H3 does not participate in the dynamic exchange of acetate modification groups (≡ 0%). The fraction of H3 calculated to be involved in this dynamic acetylation was 19%.

No.	Steady-State Acetylation for Culture Condition		[^{3}H]Acetate Pulse Label				Calculated Posttranslational Acetylation
			Fluorograph		Calculated label in		
	Mix	Photo	L = 4 h	D = 4 h	Amino acids	AcLys	
					%		
0	67.3	65.3 ± 3.1	9.2	37.2	77	≡ 0	≡ 0
1	13.3	15.0 ± 1.3	14.2	15.1	18	13 ± 1	14
2	6.7	7.6 ± 1.1	17.6	11.5	5	18 ± 1	22
3	6.0	5.5 ± 0.7	21.8	13.1	–	25 ± 1	30
4	4.2	4.2 ± 0.8	24.5	13.0	–	27 ± 1	22
5	2.7	2.4 ± 0.6	12.6	10.1	–	17 ± 3	13
AcLys/H3	0.75	0.76 ± 0.09	2.76	1.78	0.28	3.2 ± 0.1	3.0

modified forms observed in AUT gels for histone H3 and of the low levels of similar modifications in histone H4 and H2B can be established by a short pulse label with radioactive acetate (Waterborg and Matthews, 1983; Waterborg, 1990). In most cells, tritiated acetate, supplied in an acetate-free growth medium, is rapidly converted to [^{3}H]acetyl-CoA, a substrate for acetyltransferases. Typically, initial label incorporation into histones is limited to the irreversible, co-translational acetylation of the amino-terminal Ser residues of histones H1, H2A, and H4 and to the reversible posttranslational acetylation of Lys residues, located in the amino-terminal domains of core histones H3, H4, H2B, and H2A by nuclear histone acetyltransferases (Matthews and Waterborg, 1985). However, acetate will also enter into amino acid synthetic pathways and will thus be incorporated, typically after a small delay, into all newly synthesized proteins, including histones.

Exploratory experiments of the time course of acetate incorporation in vivo into *Chlamydomonas*, grown under continuous light, and thus asynchronously, in minimal medium, free of acetate, showed that tritiated acetate was effectively taken up and incorporated. AUT gel analysis by fluorography revealed that already after 10 min significant amounts of label had been incorporated into the highest mobility form of histone H3. Because histone H3 is typically free of co-translational acetylation, confirmed below for *Chlamydomonas* H3, this clearly indicates that acetate very quickly enters into amino acid pools and can be used to measure protein synthesis. When the length of the acetate pulse was extended to 60 min or longer, a significant decrease of label associated with the acetylated forms of the core histones was observed in AUT gel fluorographs.

In parallel, the distribution of radioactivity in reversed-phase HPLC elution profiles and in Coomassie blue-staining patterns of histone proteins in gels converged to that of the distribution of histone protein (results not shown). This demonstrated two important points. (a) The posttranslational acetylation of Lys's in *Chlamydomonas* core histones is highly dynamic. The rate of change from the pulse-labeling pattern to the steady-state distribution showed that, on average, the half-life of acetylated side chains is much less than 10 min and may be as low as 3 min, similar to mammalian cells (Matthews and Waterborg, 1985). (b) Radioactive acetate provides an effective way to study protein synthesis in *Chlamydomonas* when cultured in acetate-free medium. One would predict that [^{14}C]acetate would be a more effective precursor for radioactive amino acids than [^{3}H]acetate. However, [1-^{14}C]acetate is 30 times more expensive. A direct comparison between incorporation of 100 μCi [1-^{14}C]acetate and 1 mCi [^{3}H]acetate for 3 h into the histones of 200 mL of phototrophic culture (3.5×10^6 cells/mL) confirmed this expectation when the radioactivity per amount of histone *A* in the HPLC eluent was measured. However, despite a higher loss of radioactivity,

tritiated acetate yielded a 2-fold higher value of cpm per amount of histone at one-third of the price, relative to [1-^{14}C]acetate, and was used in all subsequent experiments. The steady-state acetylation of histone H3 in phototrophic cultures, measured by AUT gel electrophoresis of HPLC-purified histone, was identical with that observed under mixotrophic conditions of growth (Table I).

Cell-Cycle Analysis of Histone Synthesis

Light-dark-synchronized cultures, grown under conditions of a doubling in cell mass during the light and a single cell division during the subsequent dark period (Fig. 6A) (Harris, 1989), were incubated with tritiated acetate for 2 h to measure histone protein synthesis. Histones were extracted from isolated nuclei and fractionated by reversed-phase HPLC (Fig. 7) with determination of label incorporated into histone peaks. In addition, the specific radioactivity of all histone species, including acetylated and ubiquitinated forms, was determined after gel electrophoresis from fluorograph intensities (Fig. 8, G–L) relative to amounts of protein, as determined by Coomassie blue staining (Fig. 8, A–F). A biphasic pattern of histone synthesis was observed (Fig. 6, B–E and H–J). The same pattern was observed by northern analysis of mRNA levels for histones H3 (Fig. 6I) and H4 (Fig. 6J). The second period of synthesis coincided approximately with a doubling in the concentration of histone protein in the cultures (Fig. 8, A–F) within 6 h after the start of the dark period. It has been well established that during this time the nuclear DNA is duplicated, followed almost immediately by cytokinesis (Harris, 1989). The first period of histone synthesis, although distinct, did not cause a clear increase in histone protein levels (Fig. 8, A, D, and E). This suggests that more histone is produced during the dark. The synthetic period in the dark is at least twice as long (Figs. 6 and 8, G–L). Also, the incorporation of label into histone, relative to incorporation into nonhistone proteins, is 6-fold higher during histone synthesis in the dark (Fig. 7C) than during the light (Fig. 7A). However, this cannot be taken as a quantitative measure because the amino acid pool size most likely will be different under growth in light versus dark conditions and thus will be labeled by tritiated acetate to different levels of specific radioactivity.

Northern analysis of mRNA levels for histone H3 (Fig. 6I) and H4 (Fig. 6J) was used as an independent methodology, which would not be subject to variations in amino acid pool size or metabolic utilization of acetate. This method, too, showed that the major synthetic period of histones occurs during the dark when cell number and DNA concentration in the cultures double. The relatively low peak levels of histone mRNA during the light period support the speculation that incubation of cells with radioactive acetate under these photosynthetic conditions results in a relatively high specific radioactivity of newly synthesized histone. For both histone species a basal histone mRNA level of approximately 15%, relative to peak values, was observed (Fig. 6, I and J). Further experiments are in progress to determine whether DNA synthesis can be detected when histone mRNA levels and protein synthesis increase in the light.

Analysis of the synthesis patterns of individual histone species revealed small but significant differences. The relative intensity of labeling of the two histone H1 bands, especially clearly seen at the later times during the light period, showed that the basal level of expression of histone H1.1 was higher than that of histone H1.2 (Figs. 6, B and C, and 8G). Similarly, histone H2A.2 appears less strongly regulated in the cell cycle than the H2A.1 form (Figs. 6, D and E, and 8H). This supports the notion that all H1 and H2A forms are produced from distinct genes and that they represent primary sequence variants. Overall, considering all histone species, basal rates of histone synthesis appear significant, in the range of 5 to 20%, relative to peak rates of synthesis (Fig. 6).

Whereas synthesis of histone H2B follows the biphasic pattern seen for all histones (Figs. 6H and 8J), label incorporation into uH2B was completely different (Fig. 6G). Label incorporation into uH2B to much higher levels than H2B itself (Fig. 7B), especially immediately following the start of the light period (Fig. 8I), demonstrated that this represents de novo synthesis of the ubiquitin moiety rather than histone H2B synthesis. This pattern of ubiquitin synthesis and its conjugation to histone H2B is matched by an increase in the modification of H2B by ubiquitination during the light period (Fig. 6F). The low level of label incorporation during the dark period (Fig. 6G) is reflected in the decrease in the H2B ubiquitination level (Fig. 6F) at the same time when new H2B is synthesized (Fig. 6H). The absence of the two peaks of histone synthesis in the uH2B label pattern (Fig. 6G) and a specific radioactivity of H2B during the synthetic periods that is higher than uH2B (Fig. 6, G and H) suggests that the rate of conversion of newly synthesized histone H2B into uH2B is slow.

Acetate Pulse Labeling of Histones

Whereas the steady-state level of H2B ubiquitination varied throughout the cell cycle (Fig. 6F), no significant changes could be detected in the high steady-state levels of acetylation of histone H3, measured as 0.69 ± 0.12 (n = 11) acetylated Lys residues per histone H3 protein molecule by Coomassie blue staining (Fig. 8E) and as 0.65 ± 0.09 (n = 4) by steady-state acetate labeling (Fig. 8K). The same appeared generally true for the much lower levels of acetylation of histone H4 (0.32 ± 0.07, n = 8 [Fig. 8F], and 0.09 ± 0.02, n = 2 [Fig. 8L]), histone H2B (0.13 ± 0.03, n = 11 [Fig. 8D], and 0.11 ± 0.03, n = 7 [Fig. 8J]), or ubiquitinated histone H2B (0.23 ± 0.05, n = 11 [Fig. 8C], and 0.11 ± 0.03, n = 3 [Fig. 8I]).

To analyze the dynamic character of histone acetylation, *Chlamydomonas* cells were pulse labeled with tritiated acetate under the condition of basal histone synthesis (Fig. 9A) and during S phase (Fig. 9B). In the absence of major histone synthesis, only highly acetylated histone H3 was strongly labeled (Fig. 9A), almost exclusively in acetylated bands (Fig. 10A). Label incorporation into linker histones was not seen. Labeling of uH2B was higher than that of

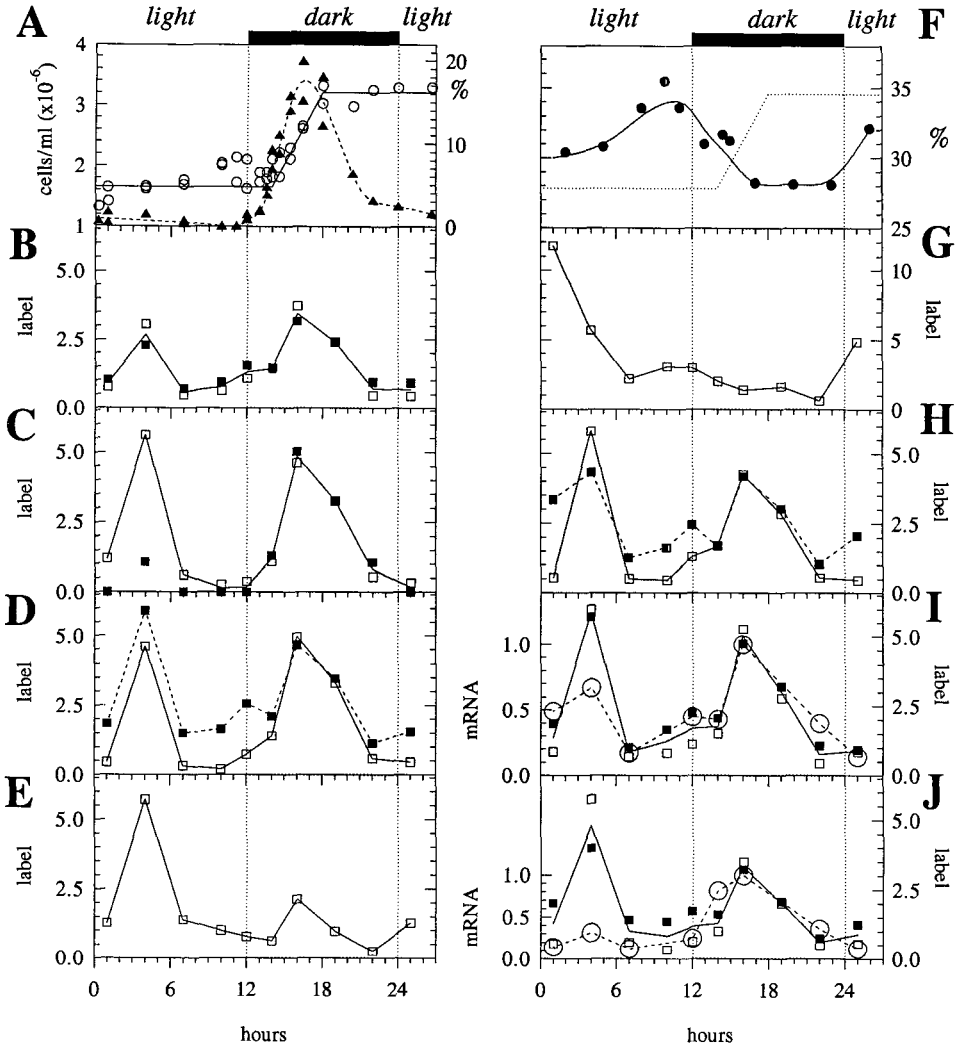

Figure 6. Histone synthesis in light-dark-synchronized *Chlamydomonas* cells. A, Increase in cell density (left axis, open circles and continuous line) of *C. reinhardtii* mutant *cw-15* cells in phototrophic cultures, cell-cycle-synchronized by an alternating 12-h light, 12-h dark regimen. The timing of cell division, and thus indirectly of the preceding phase of DNA replication, was determined by microscopic observation of cells in nonglobular, cell division-associated forms. The percentage of these cells is indicated on the right axis by the solid triangles and broken line. The dotted lines indicate the transition between light and dark conditions in this and all other panels. The timing of this panel is shown at the bottom. B, Specific radioactivity (label) of [^{3}H]acetate, incorporated in vivo in 2 h from 0.5 mCi into a 200-mL culture, described in A, into histone variant H1.1 and determined as cpm per A_{214} (solid squares) in the HPLC eluent of histone fractionation (see Fig. 7) and from the fluorographic density (Fig. 8G) and Coomassie blue staining (Fig. 8A) in SDS gels (open squares). The numerical values of both types of measurements of specific radioactivity were averaged to allow recalculation (A–J) into one arbitrary scale that allowed comparison of the results by the different methods and among the different panels with measurements for other histone species. The time of each sample corresponds to the middle of the period of incubation with tritiated acetate. C, Specific radioactivity (label), as in B, for histone variant H1.2, determined by HPLC (solid squares) and SDS gel (open squares) analysis. Early-light HPLC values were highly inaccurate because of high levels of label incorporation into nonhistone proteins (Fig. 7, A and B). D, Specific radioactivity (label), as in B, for total histone H2A by HPLC analysis (solid squares with broken line) and for histone variant H2A.1 by AUT gel analysis (open squares with line). E, Specific radioactivity (label), as in B, for histone variant H2A.2 by AUT analysis (open squares with line). F, Steady-state level of histone H2B ubiquitination, determined from the relative *A* of H2B and uH2B peaks (Fig. 7) in the HPLC eluent. By dotted lines the transitions between light and dark periods and the pattern of cell density (A) are indicated. G, Specific radioactivity (label), as in B, for ubiquitinated histone H2B by AUT analysis (open squares with line). H, Specific radioactivity (label), as in B, for total histone H2B by HPLC analysis (solid squares with broken line) and for nonubiquitinated histone H2B by AUT gel analysis (open squares with line). I, Specific radioactivity (label), as in B, for histone H3, determined by HPLC (solid squares) and AUT gel (open squares) analysis. The relative level of a histone H3-specific hybridization signal in northern analysis (open circles with broken line) is indicated on the left axis (mRNA). J, Specific radioactivity (label), as in B, for histone H4, determined by HPLC (solid squares) and AUT gel (open squares) analysis. Histone H4 mRNA level (mRNA), as in I, determined by H4-specific northern analysis (open circles with broken line).

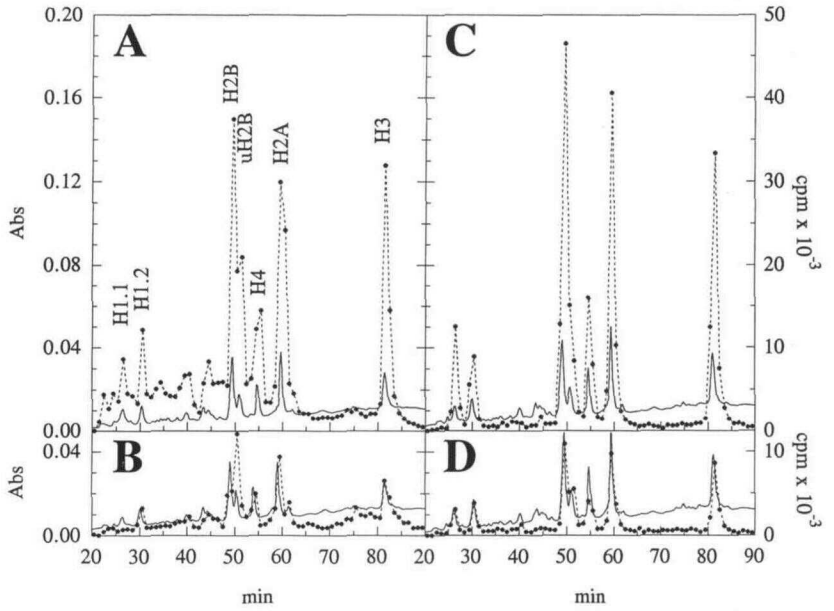

Figure 7. HPLC patterns of histone synthesis in synchronized cells. A, A_{214} pattern (line and left axis) in the reversed-phase HPLC eluent of histones, cultured and labeled with tritiated acetate, as described for Figure 6. The total radioactivity, incorporated in 1-mL fractions between 3 and 5 h after the start of light (L = 3–5 h), is shown by solid circles on a broken line (right axis). The identified histone species are marked as in Figure 3. B, Incorporation of radioactivity in 2 h, prior to the start of histone isolation at L = 11 h, in culture as in A. C, Incorporation of radioactivity in 2 h, prior to the start of histone isolation at dark (D) = 5 h, in culture as in A. D, Incorporation of radioactivity in 2 h, prior to the start of histone isolation at D = 11 h, in culture as in A.

unmodified H2B, reflecting the high rate of ubiquitin synthesis at this time (Fig. 9A). AUT gel fluorographs of histones H4 and H2B demonstrated that the charge-modified bands of these histones represented posttranslational acetylations. However, the label incorporation into acetylated bands was modest relative to label in the unmodified forms. This matches the low steady-state levels of acetylation of these histones reported above. Acetylation of the H2A variants was not detected (results not shown).

Comparison of the pattern of incorporation of tritiated acetate into histone H3 during an incubation of 5 min under conditions of basal (Fig. 9A; Table I) and high (Fig. 10C; Table I) rates of histone synthesis showed that the distribution of highly acetylated histone H3 forms was

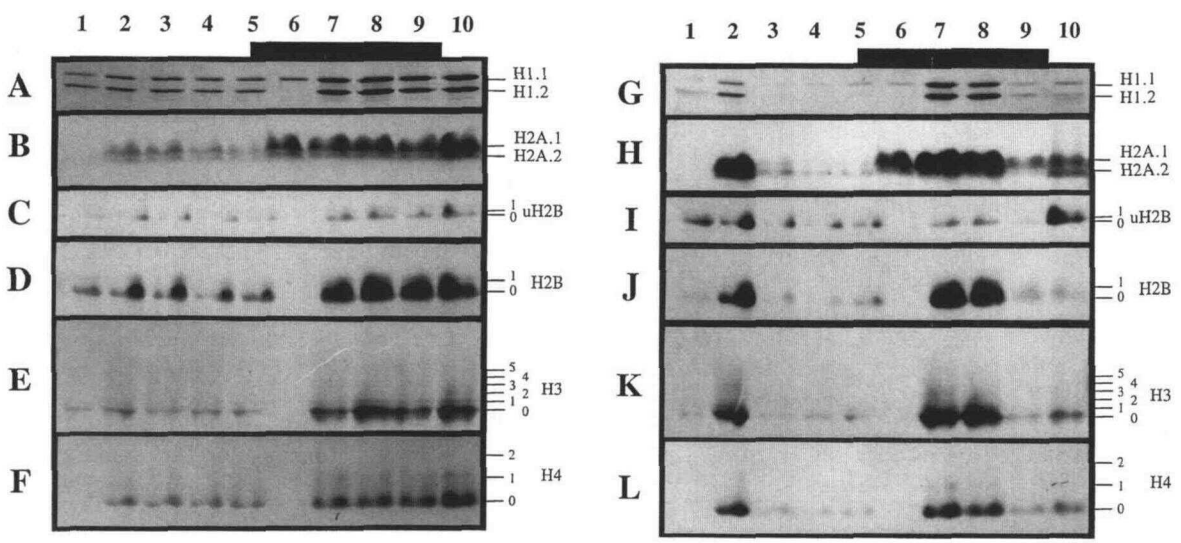

Figure 8. Gel analysis of histone synthesis in synchronized cells. Coomassie blue-staining pattern (A–F) and corresponding fluorography pattern (G–L) of histones, labeled with tritiated acetate, as described for Figure 6, and pooled based on *A* and radioactivity profiles during HPLC histone fractionation (Fig. 7). Labeling for 2 h was light = 0–2 h (lane 1), light = 3–5 h (lane 2), light = 6–8 h (lane 3), light = 9–11 h (lane 4), light = 11 h to dark = 1 h (lane 5), dark = 1–3 h (lane 6), dark = 3–5 h (lane 7), dark = 6–8 h (lane 8), dark = 9–11 h (lane 9), and light = 0–2 h (lane 10). A, SDS gel separation of histone variants H1.1 and H1.2, marked on right. Note that a pooling error caused the loss of H1.2 in lane 6. B, AUT gel separation of histone variants H2A.1 and H2A.2, marked on right. C and D, Parts from the same AUT gel that separated uH2B (C) from non-uH2B (D). The visible steady-state monoacetylated forms (1) are marked above the nonacetylated species (0). Note that a pooling error caused the loss of all H2B, H3, and H4 histones in lane 6. E, AUT separation of histone H3 into non- through penta-acetylated forms (numbered on right). F, AUT gel separation of histone H4 into non- (0), mono- (1), and diacetylated forms (2).

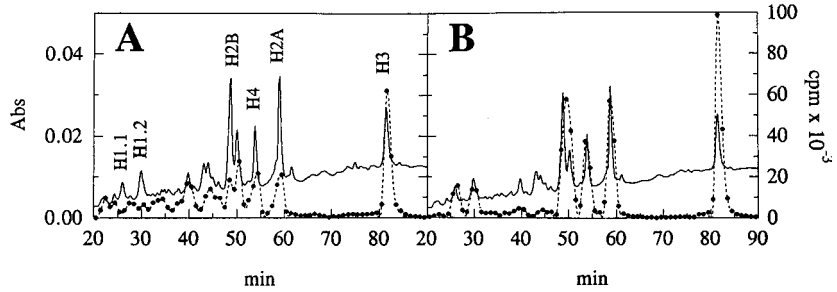

Figure 9. Acetate pulse labeling of synchronized *Chlamydomonas* cultures. A, HPLC patterns of histone synthesis in 200 mL of synchronized cells (Fig. 6A), pulse labeled at light = 5 h for 5 min with 2 mCi of [^{3}H]acetate. A_{214} pattern in the reversed-phase HPLC eluent is shown as a line (left axis). The radioactivity, incorporated in 1-mL fractions, is shown by solid circles on a broken line (right axis). The identified histone species are marked as in Figure 3. B, Incorporation of radioactivity, as in A, pulse labeled at dark = 3 h.

quite comparable. The dynamic character of this pattern was clearly demonstrated by its disappearance when the time of incubation was extended. The fluorography patterns then show steady-state patterns of histone H3 that reflect only the low (Fig. 10B) and high (Fig. 10D) rate of histone synthesis. The pulse-label comparison (Fig. 10C) allows one to assess the pattern of acetylation of newly synthesized histone H3. Apparently, new histone H3 is barely acetylated with, on average, only 0.28 acetyl-Lys groups per protein (Table I). Correction of the pulse-labeling pattern for low (Fig. 10A) and high (Fig. 10C) rates of histone H3 synthesis showed that dynamically acetylated histone H3 contained, on average, 3.2 acetylated Lys's per molecule (Table I). When the steady-state pattern of histone H3 acetylation (Fig. 5; Table I) was deconvoluted by the same method, it was found that the steady-state highly acetylated histone H3 represented 19% of total histone H3 with the same distribution and level of acetylation that was detected by acetate pulse labeling (Table I).

Sequence Analysis of Histone H3

Histone H3 (0.85 nmol), purified from mixotrophic culture, was subjected to automated Edman degradation protein sequence analysis for 50 cycles. The primary protein sequence for residues 1 through 48 was obtained (Fig. 11). This sequence was identical with that predicted from sequencing histone H3 genes in *Chlamydomonas* (GenBank accession Nos. U16724, U16725, and U16825). Analysis of the phenylthiohydantoin-amino acid derivatives, generated during the Edman degradation cycles, by HPLC allowed positive identification and quantitation of posttranslational modification of Lys by acetylation and methylation (Waterborg, 1990). Significant levels of acetylation were observed for Lys's 9, 14, 18, 23, and 27 and of N^{ϵ}-monomethylation for Lys's 4, 9, 27, 35, and 36 (Table II). Di- and trimethylated Lys was not detected. This is consistent with amino acid analysis results previously reported by Morris et al. (1990) as detectable monomethyl-Lys in *Chlamydomonas* histone H3 and H4 and confirmed by us. The average level of 0.63 acetyl-Lys moieties per histone H3 molecule, calculated from the degree of modification at each site, was very similar to the value of 0.75 obtained from AUT gel densitometry (Table I). However, it should be noted that this is only half the average level of 1.5 N^{ϵ}-monomethylated Lys's per histone H3 protein.

DISCUSSION

Chlamydomonas Histone Complexity

In this paper we present an analysis of the histone proteins of *C. reinhardtii*. The H2A gene in the cloned and sequenced histone *ch-iv* gene cluster (GenBank accession No. U12726) of *Chlamydomonas* predicts a gene product with a slightly longer carboxy-terminal tail than the H2A genes in the *ch-ii* (GenBank accession No. U16724) and *ch-iii* (GenBank accession No. U16725) clusters (Fabry et al., 1995). This may be the basis for the small size difference observed between the H2A.1 and H2A.2 protein variants (Figs. 1 and 2C). Sequence microheterogeneity among the H2B genes in these clusters may be the basis for the minor core histone species (X) with Triton affinities similar to H2B (Figs. 2D and 4B) but smaller molecular weights (Fig. 4A) that co-eluted with histone H2B and uH2B in reversed-phase chromatography. The absence of sequence heterogeneity among the three histone H3 and three histone H4 genes, sequenced from gene clusters *ch-i* (GenBank accession No. U16825), *ch-ii* (GenBank accession No. U16724), and *ch-iii* (GenBank accession No. U16725), is consistent with the detection of single forms of these proteins (Figs. 1 and 2). Identification of the two forms of histone H1 of *Chlamydomonas* as primary sequence variants was based on the difference in synthesis patterns in the cell cycle (Figs. 6 and 8G). This observation showed that H1.2 could not be a proteolytic degradation product of the histone H1.1 band. To our knowledge, only a single *Chlamydomonas* histone H1 gene has been sequenced as part of histone gene cluster *ch-iv* (GenBank accession No. U16726). It has a predicted protein size of 25 kD, like the 26-kD histone vH1-II of *Volvox*. The histone H1 gene, equivalent to the 29-kD histone vH1-I variant of *Volvox*, has not yet been cloned (Fabry et al., 1994).

Variations in the relative steady-state amounts of the two linker histone proteins and in the relative amounts of the H2A variants have been observed under different growth

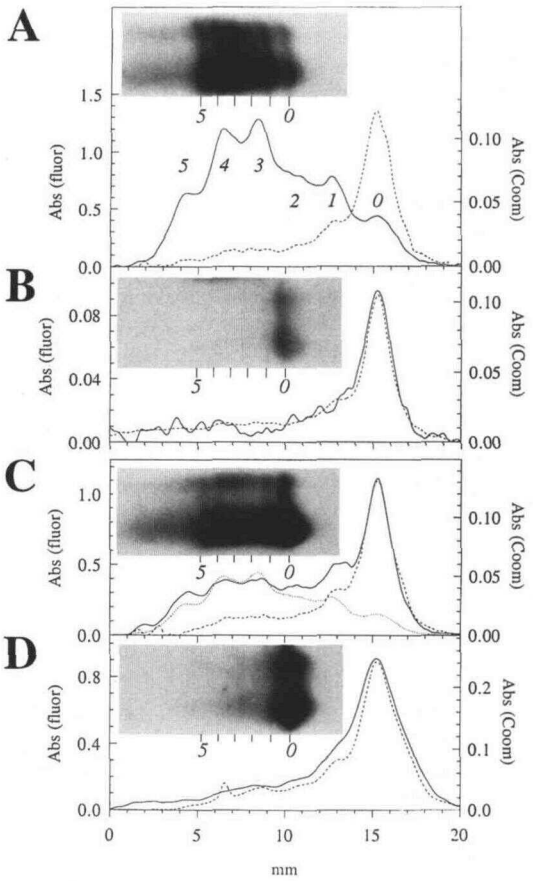

Figure 10. AUT gel analysis of acetate-labeled histone H3. A, Densitometric pattern of Coomassie blue stain [broken line, right axis, marked Abs(Coom)] and fluorography [continuous line, left axis, marked Abs(fluor)] of histone H3 in AUT gel, incubated at light = 5 h for 5 min with [^{3}H]acetate and purified by HPLC, as described for Figure 9A. The inset shows the AUT fluorography pattern of pulse-labeled histone H3 with electrophoresis from left to right. Non-through penta-acetylated forms in scans and inset are numbered. B, Analysis, as in A, of histone H3, labeled from light = 5 h to light = 7 h, in a similar experiment as described in Figure 6. C, Analysis, as in A, of histone H3, labeled for 5 min at dark = 3 h, as described for Figure 9B. D, Analysis, as in C, of histone H3, labeled from dark = 3 h to dark = 5 h.

conditions. For instance, in photosynthetic culture the more predominant forms are H1.2 (Fig. 8A) and H2A.1 (Fig. 8B), whereas in mixotrophic cultures H1.1 (Fig. 2A) and H2A.2 (Fig. 2C) are more abundant. These differences are consistent with the relative rates of basal versus replication-dependent synthesis (Fig. 6). Histone H1.1 and H2A.2, histone variants with relatively high basal rates of synthesis, were more abundant under the slower mixotrophic growth conditions (Fig. 2A).

The level of ubiquitination of H2B is high in transcriptionally active chromatin of mammalian cells when transcription is maintained and decreases when transcription is inhibited (Davie and Murphy, 1994). In photosynthetic cultures, protein synthesis and, presumably, gene transcription are strongly reduced when the lights go out. This was shown by the sharp decrease in acetate label incorporation into nonhistone proteins (Fig. 7). At the same time we observed a decrease in the steady-state level of H2B ubiquitination, which recovered when the next light period started and protein synthesis resumed (Fig. 6F). This may reflect the ubiquitination of H2B in transcriptionally active chromatin. The high influx of newly synthesized ubiquitin into uH2B (Fig. 6G) and a steady-state acetylation level that is twice that of non-uH2B are consistent with this interpretation. Fractionation studies of *Chlamydomonas* chromatin are in progress to confirm the expected preferential localization of uH2B in transcriptionally active chromatin.

Radioactive Acetate Labeling of Histones

Incubation of photosynthetic cultures of *Chlamydomonas* with radioactive acetate was used to establish two distinct aspects of histones. Histone synthesis could be studied when acetate was present for more than a few minutes. Entry of externally added acetate into the cell metabolism and conversion into amino acids, used in de novo protein synthesis, is fast. This was clearly demonstrated by the strong labeling of newly synthesized, nonacetylated histone H3 after only 5 min of incubation during a time when the rate of histone synthesis was high (Fig. 10C). When the time of incubation was extended to 1 h or more, the pattern of radioactivity closely matched that of the steady-state pattern of protein, as measured by *A* in HPLC eluates (Fig. 7C) or by Coomassie blue staining in gels (Figs. 8, G–L, lanes 7 and 8, and Fig. 10, B and D). However, the steady-state pattern of acetate label incorporation does not precisely reflect relative rates of histone protein synthesis. In general, there exists a fair correlation, as shown by the similarity during S phase of cpm incorporated per amount of preexisting histone protein among almost all histone species (Fig. 6, C, D, H, and I). Only the more cell-cycle-independent histone H1.1 (Fig. 6B) and H2A.2 (Fig. 6E) variants fit this correlation less clearly. The correlation does not hold up when distinct metabolic conditions, growth in the light versus culture in the dark, are compared. During photosynthetic growth in the light, tritiated acetate appears to enter effectively into synthetic metabolic pathways that produce radioactively labeled amino acids reflected in the high level of label incorporation into nonhistone proteins (Figs. 7, A and B, and 9A). Such incorporation is not seen under dark conditions (Figs. 7, C and D, and 9B). This suggests that in the dark much less of the acetate supplied enters into anabolic pathways, presumably because it is used to a larger extent as a source of energy. The result of this difference is that the apparent rate of histone synthesis during the early hours of the light period in light-dark-synchronized cultures is exaggerated (Fig. 6). A more realistic view of histone synthesis rates in light and dark synthetic periods is probably provided by the mRNA levels for histone H3 (Fig. 6I) and H4 (Fig. 6J).

The reason for the distinct but small amount of histones produced in the early hours of light in light-dark-synchronized cultures is not clear. We speculate that histone synthesis during S phase in the dark without a continuous supply of metabolic energy is limited. Thus, replicated

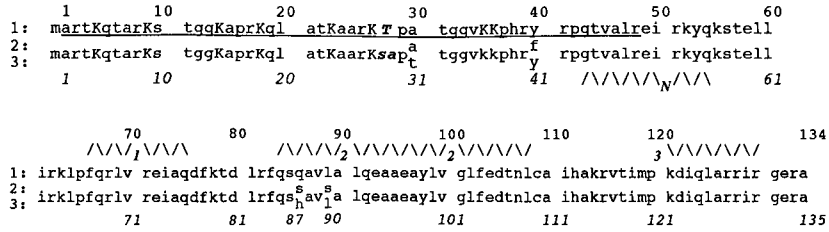

Figure 11. Histone H3 sequences of *Chlamydomonas* and alfalfa. The amino-terminal sequence of *Chlamydomonas* histone H3, residues 1 to 48, was determined by protein sequencing (underlined). It is shown superimposed on the numbered histone H3 sequence (marked as sequence 1) predicted from histone H3 gene sequences of *Chlamydomonas* (GenBank accession No. U16724). The sequences of alfalfa histone H3.1 (sequence 2) and H3.2 (sequence 3) are shown aligned as representatives of plant replication-dependent and replacement H3 histones, respectively (Waterborg, 1990). The standardized residue-numbering system for histone H3 proteins with 135 amino acids in the mature protein and with the Met initiator amino acid numbered as 0 is shown below the sequences in italics. The major sequence difference of *Chlamydomonas* Thr[28], relative to plant and animal histone H3 residues Ser[28] and Ala[29], is highlighted by bold italics. Lys residues modified by acetylation and/or methylation (Table II) (Waterborg, 1990) are shown in uppercase letters. The location of the histone H3 α-helices, the N-helix (*N*), helix-1 (*1*), helix-2 (*2*), and helix-3 (*3*) (Arents et al., 1991), are marked by the zig-zag symbols.

DNA may be packaged into chromatin using histones, newly synthesized in the dark, but the nucleosomal density of this chromatin may be less than optimal. When active growth resumes in the light, this deficit may be corrected. Similar short periods of histone synthesis, not correlated with DNA replication, have been observed in *Chlamydomonas* and the related alga, *Volvox carteri*. *Chlamydomonas*, grown under a 15-h light and 9-h dark regimen with DNA synthesis and a major period of histone synthesis in the dark, has a short period of histone synthesis in the light, demonstrated by histone H2B northern analysis, under limiting conditions of nitrogen starvation (Bulté et al., 1994). In an analogous way, light-dark-synchronized cultures of *Volvox* have a major period of histone synthesis during DNA replication, followed a few hours later, at the time when flagella are produced, by a short period of renewed histone synthesis, as shown by northern analysis for histone H1 (Fabry et al., 1994).

Table II. *Analysis of histone H3 modifications by sequencing*

Modified residues within the amino-terminal 48 residues of *Chlamydomonas* histone H3, as determined by automated protein sequencing. Dimethyl- and trimethyl-Lys residues were not detected (Waterborg, 1990). The accuracy of methylation levels for Lys residues 35 and 36 was lower than for the other residues, because of reduced levels of remaining protein caused by repetitive yield losses. At the bottom of the AcLys column, the calculated average number of acetylated Lys residues per histone H3 protein molecule (AcLys/H3) is given. AcLys, N^{ϵ}-acetyl-Lys; MMLys, N^{ϵ}-monomethyl-Lys.

Residue	Lys	AcLys	MMLys
		%	
4	18.8	0.0	81.2
9	73.2	11.2	15.6
14	83.1	16.9	0.0
18	88.9	11.1	0.0
23	83.8	16.2	0.0
27	67.5	7.3	25.2
35	75.0	0	25
36	95.0	0	5
AcLys/H3		0.63	

The variation between the peak rate of histone synthesis and the lowest, basal levels observed during the cell cycle is limited (Fig. 6). Depending on histone species or variant and on the method of analysis, basal histone rates vary from less than 5% for H1.2 (Fig. 6C) or H2A.1 (Fig. 6D) to 30% for H2A.2 (Fig. 6E). Basal mRNA levels of approximately 15% were observed for histones H3 (Fig. 6I) and H4 (Fig. 6J) in northern analyses. This range is smaller than the factor 20 to 50, observed for histones in synchronized higher animal and plant cells in culture (Osley, 1991; Kapros et al., 1993). The degree of cell-cycle synchrony observed in our experiments (Fig. 6A) makes it unlikely that the difference is due, to a significant degree, to incomplete cell-cycle synchronization. In mammalian cells it has been observed that a large part of the tight replication dependence of histone genes is caused by a T-hyphenated stem-loop structure in the 3′ untranslated region of the poly(A)-free transcripts (Osley, 1991). S phase-specific processing and mRNA stability control resides in the interaction of this structural element with cellular elements like U7 small nuclear ribonucleoprotein. The presence of potential T-hyphenated secondary structures has been noted in the 3′ untranslated regions of poly(A)-free histone transcripts of *Volvox* (Müller et al., 1990; Lindauer et al., 1993) and *Chlamydomonas* (Fabry et al., 1995). Our data would suggest that their role in cell-cycle control of histone synthesis in algae may be less than in higher animal cells.

The second aspect of *Chlamydomonas* histones that could be studied by acetate labeling is the posttranslational, reversible modification of core histones, especially of histone H3, by Lys acetylation. Fluorography of histones, prepared from cells incubated for only a few minutes with radioactive acetate and electrophoresed in AUT gels, demonstrated that the charge-modified forms of histones H2B, H4, and H3 (Figs. 2, 5, and 10) were due to acetylation. This was confirmed by protein sequencing of purified histone

H3 when acetyl-Lys residues were identified as phenylthiohydantoin derivatives by on-line HPLC (Table II). To date, we have not experimentally tested the possibility that part of the charge modifications might be due to histone phosphorylation (Ruiz-Carrillo et al., 1975; Matthews and Waterborg, 1985; Bradbury, 1992). However, the agreement between modification levels, as determined by AUT gel analysis (Table I) and by detection of acetyl-Lys's in sequenced histone H3 (Table II), without detectable levels of phospho-Ser or -Thr derivatives, makes this highly unlikely.

The differences in steady-state acetylation between the core histones are remarkably large. Histone H3 molecules, on average, contain 0.75 acetylated Lys residues (Table I), whereas this value was only 0.3 for histone H4 and 0.1 for histone H2B, and the two histone H2A forms are not acetylated to any significant degree. Acetate pulse-labeling experiments confirmed and further emphasized this difference. The pulse-label pattern for histone H3 (Fig. 10A) is dominated by the pattern of high, dynamic acetylation of this histone. It could be deduced that the average acetylation of H3 was the result of two distinct populations of molecules. Twenty percent of histone H3 molecules are highly and reversibly acetylated with, on average, three acetylated Lys's (Table I). The remaining 80% contains less than 0.3 acetylated Lys's. Such distinction was not observed for histones H4 and H2B, even though the pulse-label fluorography pattern of acetylation showed a somewhat stronger emphasis of acetylated forms than the steady-state Coomassie blue profile (results not shown). This suggests that the majority of histone H4 and H2B, like 80% of H3, has only a low level of acetylation that is not readily labeled by radioactive acetate and thus appears to be rather stable. Thus, the majority of the chromatin in *Chlamydomonas*, as in most other organisms, has only a low level of rather stable acetylation.

The small fraction of chromatin, characterized by high, dynamic acetylation, has generally been identified as chromatin that is actively transcribed or exists in a conformation poised to do so (Matthews and Waterborg, 1985; Van Holde, 1989). In higher animal cells, characteristically, histone H4 is highly acetylated with histone H3 as a close second and low levels of acetylation of H2B and H2A (Matthews and Waterborg, 1985). In *P. polycephalum* acetylation of transcriptionally active chromatin is limited to acetylation of histones H4 and H3 to high and fairly high levels, respectively (Waterborg and Matthews, 1984). In higher plants, acetylation of histone H3 predominates. Histone H4 acetylation is fairly high, H2B acetylation is significant, and only acetylation of histone H2A forms is low (Waterborg et al., 1989; Waterborg, 1991, 1992a). This study extends this analysis to green algae in which acetylation of histone H3 is much higher than in any of these other groups of organisms, but acetylation of the other core histones is much lower. This suggests the hypothesis that an overall reduction in the number of positively charged amino-terminal Lys residues of the core histones is required to facilitate transcription of chromatin and that this goal is reached in different groups of organisms by dynamic acetylation of different combinations of histones within the nucleosome.

Sequence and Modifications of Histone H3

This study confirmed by protein sequence analysis a remarkable variation in the highly conserved primary protein sequence of histone H3 (Fig. 11), predicted from histone H3 gene sequences in *Chlamydomonas* (GenBank accession Nos. U16724, U16725, and U16825). A single Thr^{28} is observed instead of the Ser^{28} and Ala^{29} present in H3 histones of every other higher eukaryote examined. As far as amino acid side chain functionality is concerned, this change appears conserved. However, it may affect the structure of histone H3 within the nucleosome. This is suggested by the observation that Lys^{35} and Lys^{36} are methylated to a significant degree (Table II).

In all species analyzed, posttranslational modification of Lys's by acetylation and methylation has always been limited to the amino-terminal domain of the core histone (approximately 30 amino acids in the case of histone H3), as defined by NMR, protease, and x-ray crystallographic analyses (Matthews and Waterborg, 1985; Schroth et al., 1990; Arents et al., 1991; Arents and Moudrianakis, 1993). In all other aspects the posttranslational modification of the algal histone H3 in *Chlamydomonas* is very similar to that of histone H3 in higher plants. Five amino-terminal Lys residues are modified by acetylation, a level never observed in animal H3 unless after extensive treatment with the histone deacetylase inhibitor *n*-butyrate (Matthews and Waterborg, 1985). The acetyl-Lys's are clustered in the center of the amino-terminal histone domain, as in alfalfa H3s, although in a somewhat broader distribution and with less preference for Lys-14 (Waterborg, 1990). In both species this pattern may be defined by the pattern of irreversible modification of Lys's by methylation. In alfalfa, quantitative methylation of Lys^{9} and Lys^{27} in histone H3.1 limits acetylation to residues 14, 18, and 23. The broader and wider pattern of acetylation in histone H3.2 with detectable acetylation of Lys^{9} and Lys^{27} coincides with reduced methylation of these residues (Waterborg, 1990). Similarly, virtually complete methylation of Lys^{4} in *Chlamydomonas* H3 prevents acetylation.

The function of Lys methylation is unknown. It had been thought that Lys methylation might provide a hydrophobic "anchor" at the transition between the amino-terminal domains of histones H3 and H4 and their hydrophobic, globular domains (Matthews and Waterborg, 1985; Waterborg, 1993a). The absence of quantitative methylation of Lys^{20} in plant histone H4 (Waterborg, 1992b) and of Lys^{27} in *Chlamydomonas* H3, reported here, suggests that this idea is at least not generally applicable. The apparent exclusion of Lys acetylation by high levels of irreversible Lys methylation in histone H3 of alfalfa, now also observed in *Chlamydomonas*, suggests a different role for Lys methylation (Waterborg, 1990). Such a function would predict that histone H3 acetylation in transcriptionally active tissues of the cycad *Encephalartos altensteinii* would be restricted to Lys^{14}, Lys^{18}, and Lys^{23}. This prediction is based on the pattern of Lys methylation seen in the inactive cycad pollen

in which histone H3, free of acetylation, is methylated at Lys^4, Lys^9, and Lys^{27} to 20, 100, and 100%, respectively (Brandt and VonHolt, 1986). Experiments are in progress to test this hypothesis experimentally in *Chlamydomonas* by a determination of the site-specific patterns of methylation and dynamic acetylation in chromatin, fractionated into transcriptionally active and inactive preparations. If this idea has validity, at what time in the life cycle and/or cell cycle of a plant would the pattern of Lys methylation be established and how could it be propagated? Study of the temporal and spatial presence of histone methylases and their unknown substrate specificity as to preferred chromatin conformation and histone protein sequence and conformation will be required.

ACKNOWLEDGMENTS

The gracious help to this project by E.H. Harris (Chlamydomonas Genetics Center at Duke University), the technical expertise of Hou Yu Chen in the western blot identification of ubiquitinated histone H2B, and the practical support and facilities made available at the start of the project by R. Hirschberg are very much appreciated.

Received January 20, 1995; accepted June 14, 1995.

LITERATURE CITED

Arents G, Burlingame RW, Wang BC, Love WE, Moudrianakis EN (1991) The nucleosomal core histone octamer at 3.1 A resolution. A tripartite protein assembly and a left-handed superhelix. Proc Natl Acad Sci USA **88:** 10138–10148

Arents G, Moudrianakis EN (1993) Topography of the histone octamer surface: repeating structural motifs utilized in the docking of nucleosomal DNA. Proc Natl Acad Sci USA **90:** 10489–10493

Bradbury EM (1992) Reversible histone modifications and the chromosome cell cycle. Bioessays **14:** 9–16

Brandt WF, VonHolt C (1986) The primary structure of histone H3 from cycad pollen. FEBS Lett **194:** 278–281

Bulté L, Vallon O, Wollman FA (1994) *Chlamydomonas reinhardtii* response to amino-acids as a sole source of nitrogen (abstract No. 85). Presented at the Sixth International Conference on the Cell and Molecular Biology of *Chlamydomonas*, May 17–22, 1994, Tahoe City, CA

Chicoine LG, Schulman IG, Richman R, Cook RG, Allis CD (1986) Nonrandom utilization of acetylation sites in histones isolated from *Tetrahymena*. Evidence for functionally distinct H4 acetylation sites. J Biol Chem **261:** 1071–1076

Clarke DJ, ONeill LP, Turner BM (1993) Selective use of H4 acetylation sites in the yeast *Saccharomyces cerevisiae*. Biochem J **294:** 557–561

Couppez M, Martin-Ponthieu A, Sautiere P (1987) Histone H4 from cuttlefish testis is sequentially acetylated. Comparison with acetylation of calf thymus histone H4. J Biol Chem **262:** 2854–2860

Csordas A (1990) On the biological role of histone acetylation. Biochem J **265:** 23–38

Davie JR, Murphy LC (1994) Inhibition of transcription selectively reduces the level of ubiquitinated histone H2B in chromatin. Biochem Biophys Res Commun **203:** 344–350

Delcuve GP, Davie JR (1992) Western blotting and immunochemical detection of histones electrophoretically resolved on acid-urea-Triton polyacrylamide gels and sodium dodecyl-sulfate polyacrylamide gels. Anal Biochem **200:** 339–341

Durrin LK, Mann RK, Kayne PS, Grunstein M (1991) Yeast histone H4 N-terminal sequence is required for promoter activation *in vivo*. Cell **65:** 1023–1031

Fabry S, Lindauer A, Cornelius T, Huber H, Klose R, Brüderlein M, Schmitt R (1994) Examination of histone H1 genes and their gene products in *Volvox carteri* and *Chlamydomonas reinhardtii* (abstract No. 60). Presented at the Sixth International Conference on the Cell and Molecular Biology of *Chlamydomonas*, May 17–22, 1994, Tahoe City, CA

Fabry S, Müller K, Lindauer A, Park PB, Cornelius C, Schmitt R (1995) The organization, structure and regulatory elements of *Chlamydomonas* histone genes reveal features linking plant and animal genes. Curr Genet (in press)

Franklin SG, Zweidler A (1977) Non-allelic variants of histones 2A, 2B and 3 in mammals. Nature **266:** 273–275

Grunstein M (1990) Histone function in transcription. Annu Rev Cell Biol **6:** 643–678

Harris EH (1989) The Chlamydomonas Sourcebook. A Comprehensive Guide to Biology and Laboratory Use. Academic Press, San Diego, CA

Kapros T, Stefanov I, Magyar Z, Ocsovszky I, Dudits D (1993) A short histone H3 promotor from alfalfa specifies expression in S phase cells and meristems. In Vitro Cell Dev Biol **29:** 27–32

Kapros T, Waterborg JH (1995) Rapid extraction of multiple RNA samples from plant suspension cells. Focus **17:** 20–21

Keller LR, Schloss JA, Silflow CD, Rosenbaum JL (1984) Transcription of alpha- and beta-tubulin genes *in vitro* in isolated *Chlamydomonas reinhardi* nuclei. J Cell Biol **98:** 1138–1143

Lindauer A, Müller K, Schmitt R (1993) Two histone H1-encoding genes of the green alga *Volvox carteri* with features intermediate between plant and animal genes. Gene **129:** 59–68

Mann RK, Grunstein M (1992) Histone H3 N-terminal mutations allow hyperactivation of the yeast GAL1 gene in vivo. EMBO J **11:** 3297–3306

Matthews HR, Waterborg JH (1985) Reversible modifications of nuclear proteins and their significance. *In* Freedman RB, Hawkins HC, eds, The Enzymology of Post-Translational Modification of Proteins, Vol 2. Academic Press, London, pp 125–285

Megee PC, Morgan BA, Mittman BA, Smith MM (1990) Genetic analysis of histone H4: essential role of lysines subject to reversible acetylation. Science **247:** 841–845

Mende LM, Waterborg JH, Müller RD, Matthews HR (1983) Isolation, identification and characterization of histones from plasmodia of the true slime mold *Physarum polycephalum* using extraction with guanidine hydrochloride. Biochemistry **22:** 38–51

Morris RL, Keller LR, Zweidler A, Rizzo PJ (1990) Analysis of *Chlamydomonas reinhardtii* histones and chromatin. J Protozool **37:** 117–123

Müller K, Lindauer A, Brüderlein M, Schmitt R (1990) Organization and transcription of *Volvox* histone-encoding genes: similarities between algal and animal genes. Gene **93:** 167–175

Munks RJL, Moore J, ONeill LP, Turner BM (1991) Histone H4 acetylation in *Drosophila*. Frequency of acetylation at different sites defined by immunolabelling with site-specific antibodies. FEBS Lett **284:** 245–248

Nickel BE, Allis CD, Davie JR (1989) Ubiquinated histone H2B is preferentially located in transcriptionally active chromatin. Biochemistry **28:** 958–963

Osley MA (1991) The regulation of histone synthesis in the cell cycle. Annu Rev Biochem **60:** 827–861

Pesis KH, Matthews HR (1986) Histone acetylation in replication and transcription: turnover at specific acetylation sites in histone H4 from *Physarum polycephalum*. Arch Biochem Biophys **251:** 665–673

Ruiz-Carrillo A, Wangh LJ, Allfrey VG (1975) Processing of newly synthesized histone molecules. Nascent histone H4 chains are reversibly phosphorylated and acetylated. Science **190:** 117–128

Sambrook J, Fritsch EF, Maniatis T (eds) (1989) Molecular Cloning. A Laboratory Manual, Ed 2. Cold Spring Harbor Laboratory, Cold Spring Harbor, NY

Schroth GP, Yau P, Imai BS, Gatewood JM, Bradbury EM (1990) A NMR study of mobility in the histone octamer. FEBS Lett **268:** 117–120

Shimogawara K, Muto S (1992) Purification of *Chlamydomonas* 28-kDa ubiquitinated protein and its identification as ubiquitinated histone H2B. Arch Biochem Biophys **294:** 193–199

Thorne AW, Kmiciek D, Mitchelson K, Sautiere P, Crane-Robinson C (1990) Patterns of histone acetylation. Eur J Biochem **193:** 701–714

Turner BM, Fellows G (1989) Specific antibodies reveal ordered and cell-cycle-related use of histone H4 acetylation sites in mammalian cells. Eur J Biochem **179:** 131–139

Van Holde KE (1989) Chromatin. Springer Verlag, New York

Waterborg JH (1990) Sequence analysis of acetylation and methylation of two histone H3 variants of alfalfa. J Biol Chem **265:** 17157–17161

Waterborg JH (1991) Multiplicity of histone H3 variants in wheat, barley, rice and maize. Plant Physiol **96:** 453–458

Waterborg JH (1992a) Existence of two histone H3 variants in dicotyledonous plants and correlation between their acetylation and plant genome size. Plant Mol Biol **18:** 181–187

Waterborg JH (1992b) Identification of five sites of acetylation in alfalfa histone H4. Biochemistry **31:** 6211–6219

Waterborg JH (1993a) Dynamic methylation of alfalfa histone H3. J Biol Chem **268:** 4918–4921

Waterborg JH (1993b) Histone synthesis and turnover in alfalfa. Fast loss of highly acetylated replacement histone H3.2. J Biol Chem **268:** 4912–4917

Waterborg JH, Fried SR, Matthews HR (1983) Acetylation and methylation sites in histone H4 from *Physarum polycephalum*. Eur J Biochem **136:** 245–252

Waterborg JH, Harrington RE, Winicov I (1987) Histone variants and acetylated species from the alfalfa plant *Medicago sativa*. Arch Biochem Biophys **256:** 167–178

Waterborg JH, Harrington RE, Winicov I (1989) Differential histone acetylation in alfalfa (*Medicago sativa*) due to growth in NaCl. Responses in salt stressed and salt tolerant callus cultures. Plant Physiol **90:** 237–245

Waterborg JH, Matthews HR (1983) Acetylation sites in histone H3 from *Physarum polycephalum*. FEBS Lett **162:** 416–419

Waterborg JH, Matthews HR (1984) Patterns of histone acetylation in *Physarum polycephalum*. H2A and H2B acetylation is functionally distinct from H3 and H4 acetylation. Eur J Biochem **142:** 329–335

Wu RS, Panusz HT, Hatch CL, Bonner WM (1986) Histones and their modifications. CRC Crit Rev Biochem **20:** 201–263